Green Chemistry

PAPER

View Article Online
View Journal | View Issue

Cite this: *Green Chem.*, 2016, **18**, 1785

All-vanadium dual circuit redox flow battery for renewable hydrogen generation and desulfurisation†

Pekka Peljo,[a] Heron Vrubel,[a] Véronique Amstutz,[a] Justine Pandard,[a] Joana Morgado,‡[a] Annukka Santasalo-Aarnio,[c] David Lloyd,[b] Frédéric Gumy,[a] C. R. Dennison,[a] Kathryn E. Toghill[d] and Hubert H. Girault*[a]

Received 14th September 2015,
Accepted 9th November 2015

DOI: 10.1039/c5gc02196k

www.rsc.org/greenchem

An all-vanadium dual circuit redox flow battery is an electrochemical energy storage system able to function as a conventional battery, but also to produce hydrogen and perform desulfurization when a surplus of electricity is available by chemical discharge of the battery electrolytes. The hydrogen reactor chemically discharging the negative electrolyte has been designed and scaled up to kW scale, while different options to discharge the positive electrolyte have been evaluated, including oxidation of hydrazine, SO_2 and H_2S. The system is well suited to convert sulfur dioxide and hydrogen sulfide to harmless compounds while producing hydrogen, with overall system efficiencies from 50 to 70% for hydrogen production.

Introduction

In this work we present an all-vanadium dual-circuit redox flow battery for hydrogen generation and desulfurisation, but firstly to place our work into a broader context, the challenges of the increased utilization of renewable energy for the grid are discussed followed by a short introduction of redox flow batteries and dual-circuit redox flow batteries.

Currently, most electricity grids are designed to match consumption with production – as additional load is added to the grid, generation stations must simultaneously ramp up to meet the demand and maintain a stable grid voltage and frequency. Due to the inherent unpredictability of consumer demand, 'reserve' generation capacity is required at all times to meet any sudden rise in demand. This is achieved by maintaining a 'spinning reserve' of excess production capacity which is capable of reacting immediately, but which is not providing any effective supply to the grid. These reserves are expensive and wasteful to operate as they consume fuel while essentially operating at zero load. It is expected that with the growing implementation of inherently less predictable renewable resources such as wind and solar, normal operation of the grid, will require ever increasing 'spinning reserves' to account for both unpredictability of demand and supply of renewable electricity.[1,2]

The output of both wind and solar power is typically highly intermittent and greater use of these sources will generate increased requirements for spinning reserves. For example, in the case of solar energy broken cloud patterns can result in megawatts of photovoltaic production capacity rapidly disappearing and then reappearing on the grid. This requires other generators on the grid to rapidly adjust their output to meet the load and maintain the frequency and line voltage. A failure to maintain stability on the grid can result in localised or even cascading power failures.

Hydrogen-powered vehicles have been recently brought to market mainly by Japanese and South Korean manufacturers (Honda, Hyundai and Toyota) due to their extended autonomy in comparison with electric cars. Clean hydrogen can be generated by water electrolysis, but only if the electricity is derived from renewable sources. Additionally, the lack of hydrogen infrastructure limits the shift to utilize fuel cell vehicles. However, production and storage of hydrogen is an excellent way to levelize the power consumed to refuel vehicles operating

[a]*Laboratoire d'Electrochimie Physique et Analytique (LEPA), École Polytechnique Fédérale de Lausanne (EPFL) - Valais Wallis, Rue de l'Industrie 17, Case Postale 440, CH-1951 Sion, Switzerland. E-mail: hubert.girault@epfl.ch*
[b]*Department of Chemistry, Aalto University, PO Box 16100, 0076 Aalto, Finland*
[c]*Department of Materials Science and Engineering, Aalto University, PO Box 16100, 0076 Aalto, Finland*
[d]*Department of Chemistry, Lancaster University, Lancaster, LA1 4YB, UK*

† Electronic supplementary information (ESI) available: Synthesis and characterization of Mo_2C supported on alumina, testing of the catalytic activity of Mo_2C supported on Denstone 2000 beads, videos of Mo_2C catalysing hydrogen evolution, operation of the hydrogen reactor, reaction of positive electrolyte with N_2H_4, SO_2 and H_2S. See DOI: 10.1039/c5gc02196k

‡ Present address: Department of Energy and Process Engineering Norwegian University of Science and Technology 7491 Trondheim Norway.

on renewable energy. In this case, hydrogen fuelled vehicles would not create an additional burden for the existing electricity grid, but instead depend on hydrogen infrastructure.[1]

The introduction of significant amounts of intermittent energy sources, such as wind and solar, is fundamentally incompatible with existing grid infrastructure and modes of operation. To achieve the goal of a shift to greater use of renewable energy, greater flexibility of the grid will be required. Large-scale electricity storage, combined with renewable production of hydrogen will be key to this transition. Local production of hydrogen could also be advantageous over centralized production, as in this way no large investments for centralized hydrogen infrastructure would be required.[1]

Currently, electrochemical energy storage in the form of batteries is considered the most promising candidates to meet the need for large-scale energy storage capacity.[3] Indeed, battery technologies have been developed and demonstrated for grid-scale applications.[3] High temperature sodium–sulfur batteries have been available at the MW scale for a number of years now and benefit from both high energy density and durability. However, the high operating temperature required by the solid electrolyte (250–350 °C)[3] complicates construction and only one manufacturer currently produces this technology (NGK, Japan). Large lithium ion battery systems are now widely marketed by a range of well-known electronics companies and have rapidly become the most commonly installed form of grid-scale energy storage.[3] Lithium ion batteries are highly sensitive to temperature and require careful thermal management, as well as cell-by-cell charge control to achieve safe operation over long periods.[4] Additional concerns exist regarding safety and cost,[4] with the recently announced Tesla Powerwall costing around 350–450 USD per kWh, which indicates that even at relatively large production volumes lithium ion batteries are too expensive to meet the need for grid-scale time-shifting.

Redox flow batteries

Redox flow batteries (RFBs) are secondary battery systems where energy is stored and released by reducing or oxidising electrochemically active species dissolved in an electrolyte solution. The system consists of an electrochemical cell, where charging and discharging reactions take place, and electrolyte storage tanks (Fig. 1).

RFBs can theoretically employ a wide range of cell redox chemistries, due to the enormous variety of soluble redox species known. The choice of redox species and solvent used affects the energy density achieved due to the solubility limits and the potential difference between the two redox reactions. A broad range of redox chemistries have been studied and demonstrated in commercial systems. By far the most common commercially used systems are: Fe/Cr, Zn/Br, and all-vanadium (V/V). A range of other chemistries that involve the formation of a second, non-liquid phase, have also been reported: all-iron (Fe/Fe), all-copper (Cu/Cu), H/Br, V/air, *etc.*[5–12]

The all-vanadium chemistry is by far the most commonly used redox system in RFBs. In a vanadium redox flow battery

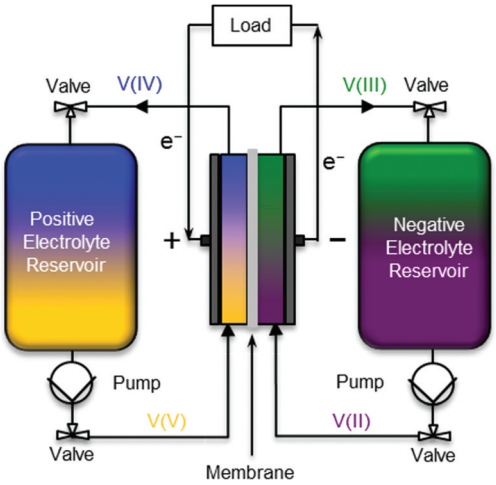

Fig. 1 System architecture for vanadium flow batteries based on liquid electrolytes.

(VRFB), the redox reactions are as shown in eqn (1) and (2). V(IV) is oxidized to V(V) in the positive half-cell during charging, simultaneously V(III) is reduced to V(II) in the negative half-cell:

$$VO^{2+} + H_2O \rightleftharpoons VO_2^{+} + 2H^{+} + e^{-}, \quad E^{\circ} = 0.991\ \text{V}\ \textit{vs.}\ \text{SHE}^{13} \tag{1}$$

$$V^{3+} + e^{-} \rightleftharpoons V^{2+}, \quad E^{\circ} = -0.255\ \text{V}\ \textit{vs.}\ \text{SHE}^{13} \tag{2}$$

The standard potentials are defined *versus* the standard hydrogen electrode (SHE).

Reaction (1) produces two protons during the charge. As protons conduct the charge through the membrane the proton concentration of both electrolytes increases by the amount of electrons transferred in the reaction. Upon discharge, the opposite reactions occur, and the proton concentration decreases in both electrolytes. In the end, the original state of the solution is reached. The standard cell potential is *ca.* 1.25 V, and as the redox potential of the solution varies with the concentration ratio of oxidized and reduced species (59 mV per decade as defined by Nernst equation), cell voltage varies from 1.1 to 1.6 V for discharged and charged state. The active vanadium species are typically dissolved in an aqueous sulfuric acid electrolyte, although other acids and acid mixtures have been used.[9,11,14] Since both electrolytes contain only vanadium species and acid, cross-over of species through the membrane is not a concern, as this leads only to chemical discharge without other adverse effects, unlike in mixed metal systems.[8,9]

The disadvantage of redox flow batteries is that the energy density of the system is limited by the solubility of the active species. Typically the concentration of active species is limited from 1 to 2 M, corresponding to an energy density of approximately 25 to 40 Wh L^{-1} of electrolyte.[8,9]

Dual-circuit redox flow battery

We have recently developed a dual-circuit redox flow battery system to bypass the energy density limitations of conventional RFBs, by adding a second 'level' of energy storage converting power to gas.[15,16] This way, electricity can be efficiently stored in the battery, but also converted to hydrogen gas through indirect electrolysis of water when the energy storage capacity of the battery has been utilized, albeit at lower efficiency. In this system, the energy capacity of the battery is not limited by the volume of the electrolytes in the reservoirs as in a conventional RFB, enabling the continuous storage of surplus renewable energy, limited only by the hydrogen storage capacity of the site. The hydrogen can be then utilized to produce electricity with fuel cells, to enrich natural gas, or directly utilized in industrial processes, but preferably to power fuel cell vehicles. It has to be stressed that the secondary mode of electricity storage is an additional unit for the battery, to be utilized only when there is a surplus of electricity available, as conventional electrolysis is more efficient for hydrogen evolution. This secondary circuit simply adds more flexibility for the system. This concept was recently demonstrated with a cerium–vanadium RFB, where the reactions upon charge are[16]

$$Ce^{3+} \rightleftharpoons Ce^{4+} + e^- \quad E^\circ = 1.72\ \text{V } vs.\ \text{SHE}^{13} \tag{3}$$

$$V^{3+} + e^- \rightleftharpoons V^{2+} \quad E^\circ = -0.255\ \text{V } vs.\ \text{SHE}^{13} \tag{4}$$

The system can function as a regular redox flow battery, so upon discharge these reactions are reversed. When surplus electricity is available, the second mode of operation can be started. In this set-up a secondary circuit was added for each half of the redox flow battery (Fig. 2), containing a catalytic reactor on both sides. The negative electrolyte is chemically discharged to produce hydrogen according to eqn (5), in case of vanadium electrolyte, and the positive electrolyte is chemically discharged in the catalytic reactor to produce oxygen according to eqn (6).

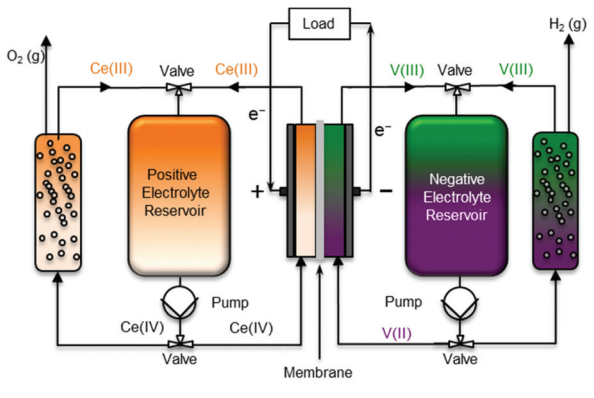

Fig. 2 Dual-circuit redox flow battery architecture. The valves allow electrolyte to pass through the external reactors, where the electrolyte may be chemically discharged 'on demand' to produce hydrogen and oxygen on the negative and positive halves, respectively.[17]

$$2H^+ + 2V^{2+} \rightarrow H_2 + 2V^{3+} \tag{5}$$

$$2H_2O + 4Ce^{4+} \rightarrow O_2 + 4H^+ + 4Ce^{3+} \tag{6}$$

The production of hydrogen consumes protons from the electrolyte solution, while oxygen evolution produces an equal amount of protons, considering a full conversion for each reaction. However, remembering that upon discharge one proton per one produced V^{3+} ion is transferred from the negative electrolyte into the positive electrolyte through the cation exchange membrane, the original states of discharged solutions are reached also by chemical discharge, consuming only water in the process.[16]

Because both hydrogen and oxygen evolution reactions are demanding proton coupled multielectron reactions, efficient catalysts are needed despite the sufficient thermodynamic potentials of the electrolytes to drive the indirect water electrolysis. RuO_2 was chosen for the oxygen evolution, because of its high catalytic activity in acidic conditions, while Mo_2C was selected for hydrogen evolution. Indirect water electrolysis by the charged electrolytes was found to proceed spontaneously in the presence of these catalysts.[16] Mo_2C was chosen because it is sufficiently active and cheap alternative for platinum.[17–19]

As the RFB utilizing the V/Ce redox chemistry suffers from some potential corrosion problems of positive electrode material and cross-mixing of V and Ce species, in this paper we focus on the concept of dual circuit vanadium redox flow battery that is both functioning as a normal RFB, but also capable of producing hydrogen when surplus electricity is available. This increases the flexibility of the battery, as now the energy storage capacity of the battery is limited by the associated hydrogen storage capability. Additionally, dual-circuit all-vanadium redox flow battery can be utilized to convert hazardous pollutants like sulfur dioxide and H_2S to more environmentally benign substances like sulfur and sulfuric acid.

Unlike in the dual-circuit cerium–vanadium redox flow battery, it is thermodynamically impossible to perform the reaction of water oxidation with V(v) solution (the standard potential E° for VO_2^+/VO^{2+} redox couple is 0.991 V *vs.* SHE[13] while the standard potential for oxygen evolution is 1.23 V *vs.* SHE[13]). Previously, the discharge of the positive electrolyte of the vanadium flow battery has been considered only from the point of view of preparation of electrolyte solutions for redox flow batteries, starting from V_2O_5. In this case, different alcohols and oxalic acid[20] have been used. Additionally, V_2O_5 is used as an oxidative agent in organic chemistry for oxidation of alcohols.[21] V(v) solution has also been used for oxidation of H_2S to sulfur, in indirect electrolysis of H_2S to produce hydrogen and sulfur from H_2S,[22] and a vanadium flow battery has been proposed for indirect preparation of Cu nanopowder by dissolution of Cu with V(v) and precipitation of Cu powder with V^{2+} electrolyte.[23,24] Additionally, it is well known that SO_2 can be oxidized with VO_2^+.[25] For our knowledge, this is the first time all-vanadium redox flow battery is proposed for hydrogen production and desulfurization.

Experimental

Chemicals

Hydrazine hydrate ($N_2H_4{\cdot}H_2O$, 50–60%), Sulfur dioxide solution (H_2SO_3, >6%), 2,4-pentanedione ($C_5H_8O_2$, >99%), 1-naphthyl red hydrochloride ($C_{16}H_{13}N_3{\cdot}HCl$, 85%), Ammonium heptamolybdate tetrahydrate ($(NH_4)_6Mo_7O_{24}{\cdot}4H_2O$, >99.9%), Sodium molybdate dihydrate ($Na_2MoO_4{\cdot}2H_2O$, >99%), Sodium sulfide nonahydrate ($Na_2S{\cdot}9H_2O$, >98%), Sulfuric acid (H_2SO_4, 95–97%) and alumina beads (3 mm) were purchased from Sigma-Aldrich and used without further purification. Dentstone beads were purchased from St-Gobain and used after washing. $MoO_2(acac)_2$ was prepared as previously described.[26] SO_2 gas (3.0) was supplied by Aga, Finland, and bubbled through sulfuric acid solution to prepare 100 mM SO_2 solution. The S(IV) concentration was confirmed by redox titration with 0.05 M $(NH_4)_2Cr_2O_7$ (Sigma-Aldrich). H_2S was generated *in situ* by reacting Na_2S with sulfuric acid in a reactor vessel. **Note that both SO_2 and H_2S are highly toxic gases that should be handled with proper care!**

Electrochemical experiments

A sandwich type flow reactor (Micro Flow Cell, Electrocell) was used as a SO_2/V(v) fuel cell with commercial carbon paper and a commercial fuel cell electrode with 2.5 mg cm^{-2} of Pt deposited on carbon (E-Tek) as electrodes for the vanadium and the SO_2 side, respectively. A 10 cm^2 geometrical area FAB anion exchange membrane (Fumatech) was used to separate the electrolyte solutions, and two centrifugal pumps (Iwaki, RD-12TE24-N1V12) were used to circulate the electrolytes. The flow rate was controlled by varying the speed of the pumps, and set so that no mass transport losses were observed in the electrochemical measurements. An Autolab PGSTAT100 potentiostat was used to perform the measurements.

Synthesis of the hydrogen evolution catalyst

The most common solution to circumvent limitations related to the powder form catalysts is to deposit nanoparticles on a large (inactive) catalyst support. This support can have different shapes and may be characterized by various degrees of porosity. By increasing the porosity, more catalyst can be deposited per volume of support (as the ratio surface/volume increases).

With such considerations nanoparticles of Mo_2C were synthesized firstly on 3 mm diameter alumina beads, as described previously,[27] and in more detail in the ESI,† but this support suffered from brittleness during hydrogen evolution. Hence, the Mo_2C catalyst was supported on non-porous Denstone 2000 beads (St-Gobain, Germany) that are actually meant as support beads for a catalytic bed rather than the catalyst itself. The ceramic beads were washed and dried before use to remove any remaining small dust, and spray coated with the molybdenum precursor solution. The synthesis procedure is shown in Scheme 1. For 500 g of ceramic beads, first 4 g of $MoO_2(acac)_2$ (*i.e.* bis(acetylacetonato) dioxomolybdenum(IV)) were dissolved in 40 mL of dichloromethane, and second, an

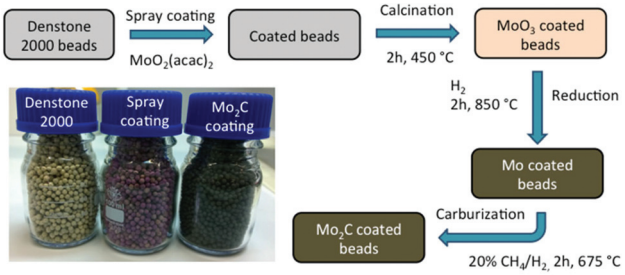

Scheme 1 Synthesis procedure of Mo_2C coated Denstone 2000 beads.

end of spatula of a dye (4-benzoazo-1-napthylamine hydrochloride) was dissolved in 80 mL of isopropanol, both being finally mixed together before being sprayed on the beads. The presence of the dye was justified by the necessity of visually controlling that the precursor is homogeneously sprayed on the support. This was followed by a calcination step, leading to MoO_3, operated in air. The temperature program began by heating up to 200 °C at the fastest available rate, then heating from 200 °C to 450 °C in a period of 2 h, followed by a constant temperature phase at 450 °C for 2 h.

The sample was then cooled down to room temperature. The reduction step to metallic molybdenum was consequently performed under a hydrogen flow, rapidly heating up to 200 °C, then from 200 °C to 850 °C in 2 h and maintaining the temperature at 850 °C for 2 h. The sample was then allowed to cool down to 675 °C. The gas flow was changed to 5–10 vol% methane in hydrogen and the catalyst was carburized in these conditions for 2 h. The sample was cooled down to 400 °C in the same gas mixture and finally the gas was changed to nitrogen until the sample had cooled to room temperature. All flows were set to approximately 1 L min^{-1}. The catalyst was then kept under nitrogen until its use. This synthesis results in grey-black beads.

Scale-up of hydrogen production

The basic platform for this development effort was a CellCube 10 kW/40 kWh all-vanadium redox flow battery produced by Gildemeister Energy Solutions (Fig. 3b). The battery was installed at a site in Martigny, Valais, Switzerland. The battery contains *ca.* 1000 L of each electrolyte, containing 1.6 M of vanadium and 2 M H_2SO_4. The roughly A4 sized single cell of the battery consists of carbon felt electrodes separated by a membrane, and compressed together by current collectors and bipolar plates. The battery contains six stacks of 20 cells in series, connected in three strings (2 stacks in series in each string, and three strings in parallel), supplying a voltage of 42–63 V and maximum currents up to 300 A in nominal conditions. The state of charge (SOC, the percentage of charge of the battery) of the battery is limited between 5 and 85% to avoid precipitation of the active species in the positive electrolyte.

The battery was retrofitted with the necessary dual circuit and catalytic reactor for hydrogen generation, and a reactor for

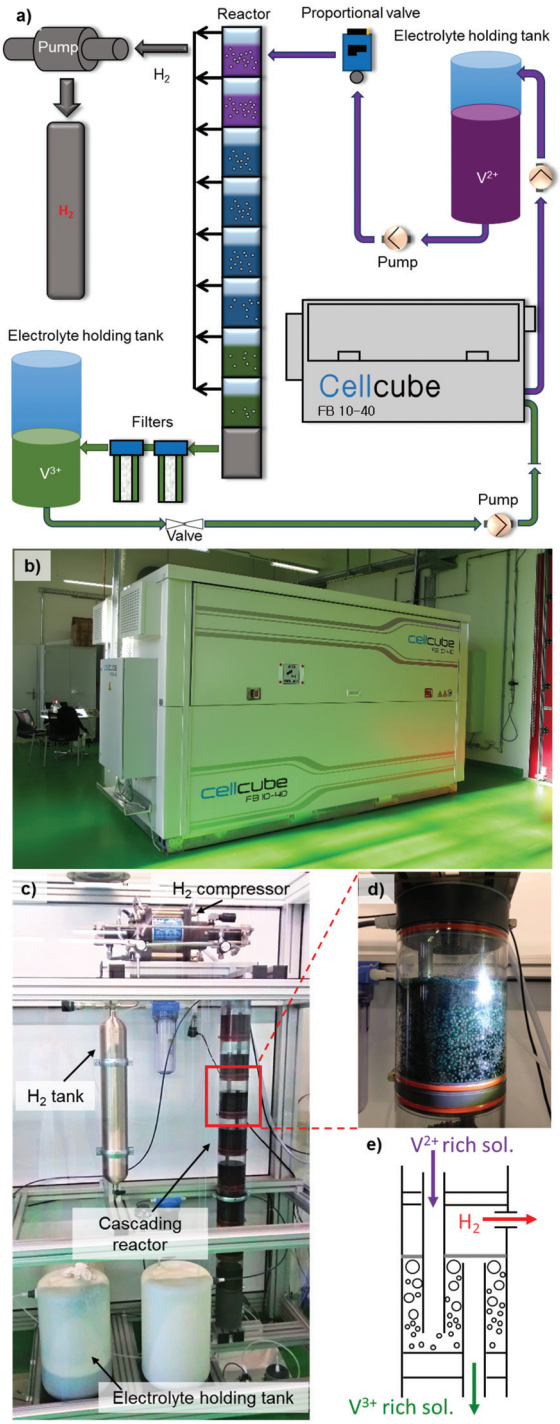

Fig. 3 (a) The flow diagram of the hydrogen reactor part of the demonstrator. (b) The demonstrator is based around a 10 kW/40 kWh all-vanadium flow battery which was retrofitted with (c) an auxiliary hydraulic circuit for producing hydrogen. (d) The reactor contains eight identical stages, where (e) the charged negative electrolyte is injected at the bottom of each stage and flows upward through the catalytic bed before reaching the outlet down to the next stage. Hydrogen is collected from the headspace of each section and compressed into the storage tank.

hydrazine oxidation. The flow chart of the hydrogen evolution part of the demonstrator is shown in Fig. 3, with the photographs of the set-up and the vertical reactor. Different reactor configurations were tested in the lab scale, with the cascade design with a fixed bed being the most satisfactory. This design was therefore selected for the scale up, constructed from transparent polycarbonate for visual inspection. The reactor itself contains eight identical stages filled with 800 g of Mo_2C catalyst supported on Denstone beads (containing in total *ca.* 16 g of Mo_2C), synthesized as described above. The electrolyte was injected to the reactor from the top, going to the bottom of each stage and flooding through the catalytic bed until reaching the exit drain going down to the next stage through a drain, as shown in Fig. 3e.

A compressed air driven diaphragm pump (SDF15 – Pump Engineering) transports the electrolyte solution from the battery into an electrolyte holding tank, and a similar pump is used to feed the reactor, with a proportional valve controlling the flow. The discharged electrolyte exits the outlet of the reactor through a gas separator and two filters to another holding tank. From there it is transferred back to the electrolyte reservoir of the battery. An equal amount of positive electrolyte is also pumped out to be discharged with hydrazine hydrate solution, and fed back to the battery.

The produced hydrogen exits from the headspace of every stage, and the operating pressure of the reactor is between 1.3 and 1.5 bar. The compressor (Haskel AGD-7-86982-ATEX gas booster) is activated when the threshold pressure of 1.5 bar is reached in the reactor, pumping hydrogen into a storage tank until the pressure of the reactor drops to 1.3 bar. The rate of hydrogen production was investigated as a function of the state of charge of the negative electrolyte, by measuring the pressure in the hydrogen storage tank. The operation of both the battery and the reactor was controlled by a LabView based software.

The discharge of the positive electrolyte was performed by a slow addition of a controlled amount of hydrazine hydrate (diluted by half in water) into the positive electrolyte holding tank. The addition was done slowly to avoid extensive heating of the electrolyte solution.

Results and discussion

All-vanadium dual circuit redox flow battery

As stated earlier, unlike in our previous concept of dual-circuit cerium–vanadium redox flow battery, it is thermodynamically impossible to perform the reaction of water oxidation with V(v) solution. Hence, other reactions needed to be evaluated. As V(v) needs to be reduced to V(iv) to discharge the positive electrolyte, a suitable oxidation reaction is required. Firstly, we will consider discharge of the negative electrolyte, followed by the discussion on discharging the positive electrolyte.

Discharging of the negative electrolyte by hydrogen evolution

Catalytic bed properties. Earlier work has shown that a sufficiently efficient catalyst is required to catalyse hydrogen

evolution from the negative electrolyte of the redox flow battery. Mo_2C was chosen as a catalyst because it is stable in acidic media under reducing condition[28,29] and not too expensive. Previously, we studied Mo_2C in the form of a powder for this reaction.[16] The size of the particles of this powder ranged from 1 to 5 μm diameter, and as a result building a fixed catalytic bed with it would lead to several issues, such as a high resistance of the catalytic bed to the electrolyte flow (requiring high pumping energies), preferential flow paths (not an optimal use of the catalyst), trapping of bubbles inside the bed (decreasing the active surface of the catalyst), and difficulty to thoroughly filter the electrolyte. Additionally, it is absolutely critical to prevent any hydrogen evolution catalyst from reaching the electrolyte reservoir of the battery to avoid uncontrollable hydrogen evolution. In order to circumvent these limitations related to the powder form of the catalyst the most common solution is to deposit nanoparticles on a large (inactive) catalyst support. In a first view, the requirements for an ideal support for the present system are:

- Chemical stability: to resist the strongly acidic media (3 M sulfuric acid) for a long-term use.
- Mechanical stability: due to the flow of the electrolyte on its surface and the formation of bubbles it has to be resistant to attrition.
- High thermal stability (up to 850 °C, at least, for the synthesis of the catalyst).
- High surface area, as it allows a high catalyst surface area per unit volume.
- Strong interactions with the catalyst, in order for the catalyst to remain adhered to the surface of the support.
- Ideally, it has to present a reactional synergy with the mechanism of the catalyst, in order to assist or promote the reaction at the catalyst surface, for instance by specific acid–base or redox properties.
- Potentially, a high electrical conductivity could be favourable, in case the catalyst mechanism implies a transfer of electron in the catalyst structure.
- A technically feasible scale-up of the catalyst synthesis process.

These requirements will be discussed along with the characterization of the synthesized support-catalyst couples. It should be noted, however, that some of these requirements were found to be mutually exclusive.

Mo_2C/ceramic catalyst. The focus for this new support was its mechanical stability and low surface area. To achieve better mechanical stability, it was decided to avoid pores as they induce a destabilisation of the support for the present reaction conditions and moreover can become blocked by hydrogen bubbles during most of the reaction time. Chemical stability was also of importance. Hence, a non-porous ceramic catalyst bed support, Denstone 2000, was chosen as a support. This material was originally designed for supporting the catalytic bed and not as catalyst support. It fulfills the requirements of the petrochemical and refinery industries, in particular for the hydrocracking reactions, performed at high pressure and subjected to high mechanical stresses. Its mechanical stability is one of its main advantages, together with its high thermal stability and chemical inertness (to avoid any poisoning of the catalyst). This oxide ceramic is composed of 74.2% SiO_2, 19.2% Al_2O_3, 2.4% K_2O, 1.7% Na_2O, 0.9% TiO_2, 0.13% CaO, 0.34% MgO, and some impurities such as Fe_2O_3 (leachable Fe <0.1%).[30] Its particle density is 2400 kg m^{-3}, whereas its packing density is 1330 kg m^{-3}. Its porosity is >5% and it has a low water absorption (2–6%). Its specific heat capacity is 1047 J kg^{-1} K^{-1} and it is stable at least up to 968 °C.[30] HRSEMs of the bare ceramic support and of the catalyst layer on top of the ceramic beads before and after the reaction are shown in Fig. 4.

It can be observed that the support presents a relatively smooth surface, free from visible pores and decorated with various structures. After the synthesis of the catalyst, this surface is fully covered by big porous particles (approximately 2 μm), very different from the catalyst obtained on the alumina support (see ESI†). It is difficult to conclude on the basis of SEM investigation if these particles are strongly attached together or not. The pores of the molybdenum carbide surface, of a size of about 200 nm were not expected and may be regarded as an issue or as beneficial, depending on the mechanical stability of the particles. Indeed, they increase the active surface area of the catalyst, but they also may induce the disintegration of the particles due to the formation of hydrogen in the pores. The experiments shown in the ESI† confirm that the Mo_2C supported on Denstone beads are efficient catalysts for hydrogen evolution. Additionally, a video of hydrogen evolution by Mo_2C supported catalysts is available in the ESI, as Video S1.†

According to the image taken after the reaction (Fig. 4d), some catalyst disintegration seems to happen, as a large part of the catalytic material left the surface of the support. However, the presence of remaining catalyst particles, even though they are smaller than after the synthesis showed that the interaction between the support and the catalyst is strong enough to endure the catalytic conditions. Furthermore, recycling the catalyst for further cycles of experiment showed that it was still catalytically active and only the first use of the catalyst decreases the quantity of catalytic material at the surface of the support. Apart from this first degradation, we see no evidence of further loss of activity. This is very common in catalysis that the first use of the catalyst leads to some deactivation due to structure rearrangements and stabilization. Only the following cycles are important. The catalyst in the reactor has now been operating for more than six months without any observable decrease in activity. The outlet of the catalytic reactor passes through a filter to retain the particles in a case of catalyst degradation, but visual inspection of the filters showed no accumulation of the particles, and the RFB has not started to evolve hydrogen in the storage tanks, indicating that the catalyst is stable. A video of the catalytic production hydrogen from the negative electrolyte of the commercial RFB is included in the ESI.† As this catalyst fulfils most of the requirements for an ideal support (although the surface to volume ratio is not very high), it was chosen as a catalyst for the hydro-

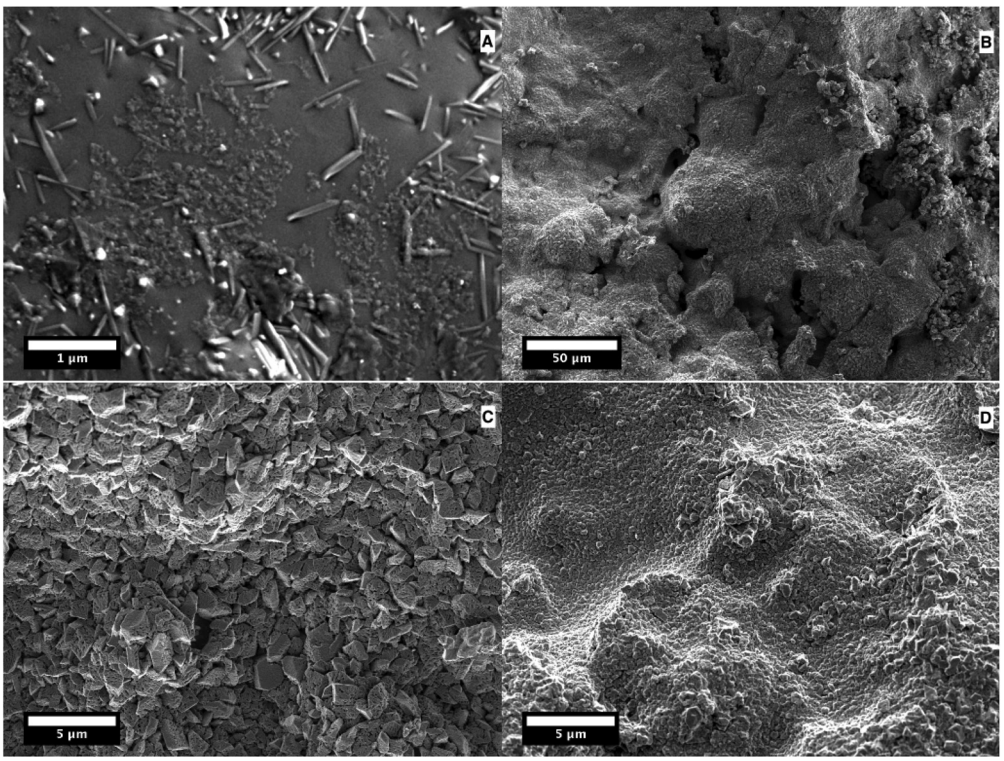

Fig. 4 HRSEM visualisation of the deposition of Mo_2C on the ceramic beads. (A) Ceramic support, (B and C) Mo_2C on the ceramic support after synthesis, (D) Mo_2C on ceramic support after use in the reaction.

gen evolution reactor of the demonstrator, and synthesized on kilogram scale.

Scale-up of the hydrogen generation

The design of the demonstrator for the dual circuit all-vanadium redox flow battery capable of indirect hydrogen generation has been described in the Experimental section. Evolution of the hydrogen volume in the storage tank for different states of charge of the electrolyte was measured at the electrolyte flow rate of 300 ml min^{-1}. The corresponding curves are shown in Fig. 5. In all these cases V^{2+} was completely converted into V^{3+} upon passing through the reactor.

These results show that the reactor is well suited for hydrogen production with full conversion of the electrolyte achieved for electrolyte flow rates up to 1 L per minute. The battery can be completely chemically discharged in 17 hours with the current design, corresponding to a conventional discharge at *ca.* 2.4 kW of power. Adding several reactor units in parallel could increase the discharge rate, if required. Indeed, the discharge rate can be tailored depending on the required power. A video of the reactor in operation is included in the ESI, as Video S2.† The steady-state rate of hydrogen production as a function of electrolyte state of charge is shown in Fig. 6.

Fig. 6 shows that there is a linear relationship between the hydrogen production rate and the state of charge of the negative electrolyte. When vanadium electrolyte is in a high state of charge, the available potential for hydrogen evolution is higher

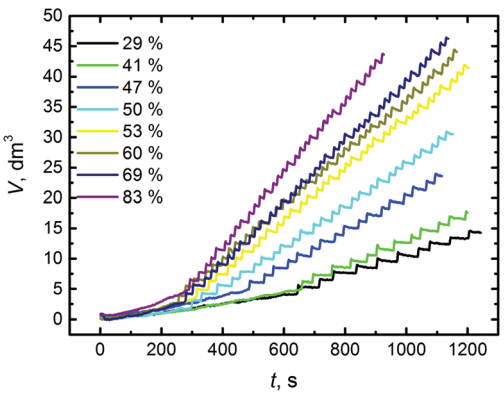

Fig. 5 Volume of produced hydrogen as a function of time for different states of charge of the negative electrolyte from the battery. The state of charge of the battery electrolytes was measured by the battery control system.

and hence the hydrogen production rate becomes higher. The highest rate correspond to an electrolysis current of *ca.* 520 A, assuming 100% efficiency for hydrogen production. This design allows the production of *ca.* 0.5 kg of hydrogen per day, but hydrogen production rate can be adjusted easily by adding more reactors in parallel. Currently, the catalyst surface is still partly covered by hydrogen bubbles, decreasing the available surface area. The catalytic bed could be further improved by

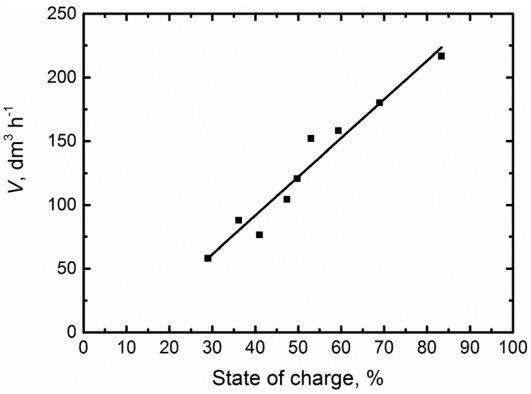

Fig. 6 The average volumetric flow of hydrogen in the reactor as the function of the state of charge of the negative electrolyte.

introducing hydrophobic channels into the reactor to facilitate release of bubbles from the catalytic bed.

Discharge of the positive electrolyte with a sacrificial electron donor/oxygen acceptor

The reaction to discharge the positive electrolyte should produce one proton per electron involved in the half-reaction in order to maintain the proton balance in each electrolyte. As a consequence, potential half-reactions include either the oxidation of a reactant while generating one proton per electron, or taking one oxygen atom from the solution, when passing from the reduced to the oxidized state. This is not self-evident, as upon charge two protons per electron are produced in an all-vanadium RFB (eqn (1)). However, one proton per electron needs to migrate through the membrane to transport the current, so the overall charging reactions increase proton concentrations in both positive and negative electrolytes of the VRFB by one proton per each electron exchanged in the electrode reaction.

Moreover, it should be practically feasible to separate the oxidized product from the positive electrolyte to avoid its accumulation and to prevent poisoning and deactivation of the battery electrodes, plugging of the whole RFB positive circuit (pumps, piping, electrodes, flow-fields,...) and blocking of the membrane. Moreover, possible changes in the electrolyte chemical composition may affect on one side the solubility of the redox active species and on the other side the OCV potential, which would imply issue for the control system. Different alternatives were explored to find an optimal solution that fulfils these requirements.

Hydrazine. The first chemical discharge reaction considered was the oxidation of hydrazine (N_2H_4) to nitrogen, according to the following half-reaction:

$$N_2H_4 \rightarrow N_2 + 4H^+ + 4e^- \quad (7)$$

The standard reduction potential of gaseous hydrazine into gaseous nitrogen can be calculated as −0.413 V *vs.* SHE from the thermodynamic data.[31] The reaction of hydrazine with V(v) was found to be spontaneous at room temperature, showing 100% conversion of hydrazine into N_2. The video of the discharge reaction is available in the ESI, as Video S3.† However, the nature of the hydrazine source is also of importance. Hydrazine in liquid form is classically in the hydrate form ($N_2H_4{\cdot}H_2O$), *i.e.* in a concentration of approximately 64 wt% in water, meaning that water will be injected in the positive electrolyte diluting it progressively. This issue is even more pronounced in reality because it was observed that hydrazine sulfate precipitates when the as-received hydrazine is injected in the electrolyte for its discharge, due to the high sulfate ion concentration. This implies that hydrazine hydrate needs to be diluted even more before being injected in the electrolyte. The use of hydrazine sulfate salt ($N_2H_5^+{\cdot}HSO_4^-$) is instead possible, but would lead to addition of sulfuric acid into the system. The kinetics of the reaction is also slower with solid hydrazine sulfate. It should be mentioned that utilization of hydrazine to produce hydrogen is not environmentally sustainable, and was only investigated as a simple way to discharge the positive electrolyte solution to allow the scale-up and further study of the hydrogen generation reaction.

Sulfur dioxide. An alternative chemical discharge reaction is the oxidation of sulfur dioxide (SO_2) by the following half-reaction:

$$SO_2 + 2H_2O \rightarrow H_2SO_4 + 2H^+ + 2e^- \quad (8)$$

The standard reduction potential of this reaction considering gaseous H_2SO_3 is 0.172 V *vs.* SHE,[13] while the standard reduction potential considering aqueous SO_2 and fully dissociated sulphuric acid has been reported as 0.158 V *vs.* SHE,[32] so this reaction is thermodynamically feasible. This reaction is an interesting solution as it allows production of a useful product, and could also be applied in some industries where SO_2 needs to be treated as a waste. The larger producers of gaseous SO_2 are mining companies extracting sulfide ores and coal power plants, but other sectors produce considerable quantities of SO_2 as well, such as petroleum refineries (desulfurization step), industrial combustion units (*e.g.* medical and/or municipal waste incinerators), glass furnaces and H_2SO_4 manufacturing facilities.[33,34] Commonly, waste SO_2 is burned and reacted with water to produce H_2SO_4, so the energy stored in SO_2 is released and partly utilized as heat.[33,34]

For the purpose of discharging the positive electrolyte, small-scale tests were performed by mixing charged positive electrolyte and SO_2. SO_2 was found to react very fast with the fully charged positive electrolyte, effectively discharging the V(v) into V(iv), as shown in the ESI Video S4.† However, the process generates sulfuric acid that has to be separated from the electrolyte. Standard sulfuric acid recovery processes like distillation or dialysis[35] could achieve this. However, distillation is very energy intensive, and would result in precipitation of the vanadium salt of the electrolyte, complicating the process. Dialysis is another option, but dialysis typically requires large areas of expensive membranes. And in both of these cases the energy from oxidation of SO_2 would be just lost

into heating the vanadium electrolyte solution. Hence, electrochemical SO_2 oxidation in a fuel cell would be preferential, allowing partial recovery of the electricity utilized in the charging of the RFB (while utilizing similar dialysis membranes). However, to recover some of the energy as electricity in a V(v)–SO_2 fuel cell, a catalyst is needed to accelerate the reaction rate of SO_2 oxidation at room temperature. Gold or platinum are the classical catalysts considered for the oxidation of SO_2,[32,36] and Pt has been predicted to be the optimum electrocatalyst by a recent DFT calculation,[37] so it was chosen as a catalyst in this study.

Electrocatalysis of SO_2 oxidation is quite complicated on all the metal surfaces. Both Au and Pt electrodes require relatively high overpotentials for the reaction, but the performance can be improved with formation of sulfur adlayers at slightly reducing potentials.[38] However, especially platinum is easily poisoned by reduction products of SO_2, requiring high enough potentials to form the surface oxide layer to recover the catalytic activity. Electrochemistry of SO_2 on gold and platinum electrodes has been recently comprehensively reviewed.[32]

The polarization curve shown in Fig. 7 was recorded as described in the Experimental section, with a carbon paper electrode for the vanadium side and Pt on carbon electrode for the SO_2 side, separated by FAB anion exchange membrane. Fuel cells typically utilize cation or anion exchange membranes to separate the electrodes. In this case, an anion exchange membrane is preferred to prevent the crossover of vanadium into the SO_2 electrolyte.

This result shows that the cell has an open circuit potential of 0.55 V, but the currents are quite modest compared to regular vanadium redox flow batteries (typically 20–200 mA cm^{-2}) The results were not significantly affected by the change of the flow rate, indicating that the performance of the cell is limited by kinetics of one of the electrode reactions. As kinetics of vanadium species are reasonably facile in redox flow batteries with current densities up to 900 mA cm^{-2} reported,[39] oxidation of SO_2 is limiting the cell performance. But as the concentrations of both V(v) and SO_2 were only *ca.* 100 mM, current and power can be increased by a factor of 10 by increasing concentrations of both electroactive species to over 1 M, increasing the maximum current densities up to 20 mA cm^{-2} and maximum power to 11 mW cm^{-2}. These currents are comparable to current densities obtained from the redox flow battery.

Additionally, cross-over of SO_2 through the membrane can be a problem, increasing the sulfuric acid concentration in the vanadium electrolyte. Cross-over of vanadium was efficiently blocked by the anion exchange membrane, whereas when a conventional cation exchange membrane was used, cross-over of both vanadium and sulfur dioxide took place at a considerable rate. However, the cross-over of SO_2 can be used as an advantage: in the current design the membrane is highly selective for only anions, so that sulfate and bisulfate ions carry the charge through the membrane. As the flux of these anions is from vanadium electrolyte into the SO_2 electrolyte, the acid concentration in the RFB circuits decreases over time. But if the SO_2/V(v) fuel cell is operated at the optimum current density so that the fluxes of SO_2 and anions match (flux of anions through the membrane is compensated by the opposite flux of SO_2), SO_2 is homogeneously oxidized by V(v) species in the vanadium electrolyte, generating sulfuric acid to compensate for the loss of the sulfate.

The conversion of SO_2 into H_2SO_4 is another concern, as not all the SO_2 is oxidized in a single pass through the fuel cell. But keeping the SO_2 solution saturated by SO_2 gas at constant pressure can solve this problem. The acidity of this solution increases as more and more SO_2 is oxidized, but when the desired concentration of sulfuric acid is reached, the inlet of SO_2 gas can be closed and all the dissolved SO_2 can be exhaustively converted into sulfuric acid. The final system is presented in Fig. 8.

The electrochemical oxidation of aqueous sulfur dioxide to sulfuric acid has been a reaction of interest in recent years due to its relevance in the hybrid sulfur cycle for large-scale hydrogen production.[32,40–43] The process aims at decreasing the potentials required to achieve water reduction to hydrogen by replacing the conventional oxygen evolution reaction at the positive electrode with the less energetically demanding oxidation of SO_2. As SO_2 oxidation occurs at much lower potentials than oxygen evolution, significantly lower cell voltages are required for hydrogen evolution. Additionally, the produced H_2SO_4 could be converted back to SO_2 in a high temperature thermochemical hybrid sulfur cycle, designed to be coupled with the heat produced by a nuclear reactor,[32,44] although the other high temperature heat sources exceeding 1000 °C could be utilized as well. However, the advantage of the current approach over conventional SO_2 oxidation depolarized hydrogen production is that the cross-over of SO_2 is not a problem. In the conventional system SO_2 cross-over results in S and H_2S production at the cathode, poisoning the hydrogen evolution catalyst and blocking the electrode with a layer of sulfur.[31] However, in the current system SO_2 crossing the membrane into the vanadium electrolyte will be chemically oxidized into sulfuric acid, as discussed earlier.

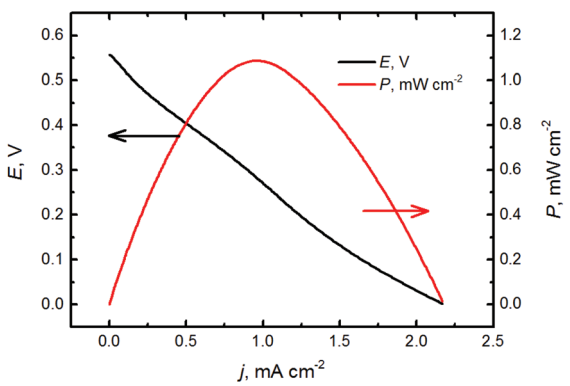

Fig. 7 Polarization curve obtained with 100 mM SO_2 in the negative electrolyte and equal amount of V(v) in the positive electrolyte, both in 2 M sulfuric acid.

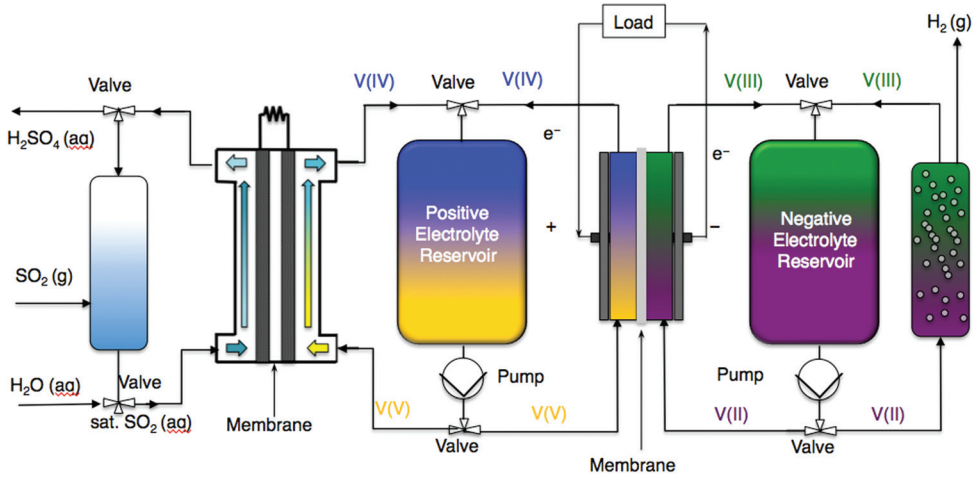

Fig. 8 Dual-circuit redox flow battery utilizing a SO_2 fuel cell for discharge of the negative electrolyte. The SO_2/V(v) fuel cell produces electricity and H_2SO_4 until an optimum level of H_2SO_4 concentration is reached. The feed of SO_2 and the remaining SO_2 in the positive dual circuit will be exhaustively electrolyzed to produce sulfuric acid. Then the circuit is drained and filled with water to be saturated further by the SO_2 feed.

The disadvantage of the present concept is that the fuel cell requires expensive components like the electrocatalyst and anion exchange membrane, so more detailed investigation of the chemical oxidation of SO_2 followed by sulfuric acid separation by dialysis *versus* the SO_2 oxidation in a fuel cell needs to be performed. As both systems utilize similar membranes, it is necessary to determine if the cost of the expensive platinum or gold catalysts is justified by the electricity recovered.

Further fundamental work is required to look for better and cheaper electrocatalysts for SO_2 oxidation, as platinum and gold can become too expensive for practical applications. If a cheaper and reasonably efficient catalyst was discovered, a fuel cell system would be preferred over the dialysis. For this purpose, we tested other promising candidates like Mo_2C[17] and MoS_2.[45] These materials have been used to successfully catalyze hydrogen evolution, and they have similar electrocatalytic properties as Pt.[46,47] Unfortunately, both Mo_2C and MoS_2 were oxidized and dissolved at *ca.* 0.6–0.8 V *vs.* SHE in 1 M H_2SO_4, and no significant differences were observed in the voltammetry in 100 mM SO_2 and 1 M H_2SO_4. Further work to identify better catalysts is required.

Hydrogen sulfide. Another alternative reaction for the chemical discharge of V(v) is the oxidation of hydrogen sulfide (H_2S) in the following half-reaction:

$$H_2S \rightarrow S + 2H^+ + 2e^- \quad (9)$$

The standard reduction potential for the reduction of sulfur to H_2S dissolved in water is 0.142 V,[13] therefore the reaction is thermodynamically feasible. The product of this discharge reaction is solid sulfur, which could be separated by filtration or decantation processes for instance. When H_2S generated by dissolution of Na_2S in sulfuric acid was bubbled through a V(v) solution, it was quickly oxidized to small sulfur particles, effectively discharging the positive electrolyte into V(iv) (the video of the discharge reaction is available in the ESI, as Video S5†). During the reaction the solution becomes turbid, indicating the formation of small sulfur particles. Additionally, although further oxidation of H_2S to sulfuric acid is thermodynamically feasible, elemental sulfur did not react with V(v) solution, confirming that the reaction is kinetically very limited. After the reaction solid sulfur can be seen floating at the surface of the solution. As with SO_2, this reaction could be useful for the industries which need to treat such a gas, as in a desulfurization process. For example, desulfurization of hydrocarbons produces H_2S in large quantities. It is to be noted that H_2S and SO_2 oxidation reactions could also be coupled in one process of desulfurization of gas, as they are often mixed in waste gas of industries.

Full system and efficiency calculations

To maintain the charge balance of the battery, equal amounts of positive and negative electrolytes need to be chemically discharged. At this stage the discharge of the positive electrolyte was done with the addition of hydrazine hydrate. The reaction takes place fast, and heats up the solution, so certain care had to be taken upon reduction of the positive electrolyte. Of course, hydrazine cannot be a final solution as it is not economically viable to produce hydrogen from hydrazine. But this provided us a convenient way to balance the state of charge of both electrolytes while studying hydrogen evolution reaction in detail.

For an optimum system, the rate of the indirect hydrogen production must be matched by the rate of indirect discharge of the positive electrolyte, otherwise the battery will become imbalanced, restricting its performance. Hence, the rate of oxidation of the positive electrolyte must match the currents required to produce hydrogen at a rate of 220 dm^3 h^{-1} (Fig. 6). This corresponds to a current of 520 A at 100% efficiency. To match this current with the SO_2 fuel cell, a stack

operating at the optimum current density of 10 mA cm^{-2} would require 90 cells of the size currently utilized in the RFB, and operation at closed circuit conditions would half the number of cells to 45. Considering that the current RFB set-up utilizes in total 120 cells, performance of the fuel cell should be drastically improved.

From the engineering point of view, both hydrazine and hydrogen sulfide form products that are easy to separate, while SO_2 oxidation produces sulfuric acid that would require separation by expensive dialysis process. Hence, chemical discharge with hydrogen sulfide would be preferred over SO_2 oxidation, but the system efficiencies have to be also considered.

To evaluate the efficiencies of the different options, the most common way is to compare the heat available from combustion of the produced fuel to the energy required to produce it. Typically, higher heating value (HHV) and lower heating value (LHV) are used for these calculations, representing the energy released when the reactants initially at 25 °C are combusted to products at 25 °C (HHV) or 150 °C (LHV). The calculation of these values is presented in the ESI.† At the hydrogen production rate of 10 mol h^{-1} (corresponding to 220 dm^3 h^{-1} of hydrogen in the STP conditions) the energetic value of hydrogen (HHV) produced in one hour would be 2.86 MJ. The experimental measured amount of energy required to recharge the discharged electrolytes with our RFB is 2.65 MJ considering only DC electricity (or 2.74 MJ of AC electricity). Typically the all-vanadium RFB has a coulombic efficiency close to 100%, and energy efficiencies up to 80% depending on charge and discharge rate. However, the overall efficiency of the system depends strongly on the reaction used to discharge the positive electrolyte. This can be accounted by considering the efficiency as a ratio of energy output *versus* energy input. The input energy contained in N_2H_4, SO_2 or H_2S is considered to equal HHV or LHV for the combustion of these reactants. The hydrogen production efficiencies of the dual circuit all vanadium battery for different cases are summarized in Table 1, considering both AC and DC electricity, chemical discharge of the positive electrolyte with reactants and electrochemical discharge of the positive electrolyte in the SO_2/V(v) fuel cell.

The results show that electrochemical discharge of the positive electrolyte with an SO_2/V(v) fuel cell gives the best efficiency of 67–69% (HHV), followed by chemical discharge of SO_2, H_2S and N_2H_4. If LHV efficiencies are considered instead, fuel cell system is still the most efficient at 61 to 62%, but now efficiencies of the system with chemical discharge of SO_2, H_2S are similar, with hydrazine as the weakest candidate. This analysis excludes the energy consumption of operating the secondary circuits.

From the practical point of view, the system costs are an important issue, and the economics of the system will be a subject of a further study, but we currently believe that if somebody invests in a RFB, the added flexibility of the dual circuit energy storage system will be worth the additional investment. The cost of the hydrogen reactor is not prohibitive, as molybdenum is used as a catalyst instead of highly expensive platinum. However, the option of electrochemical discharge of the SO_2 will most likely not be profitable due to the demand for expensive ion exchange membrane and Au/Pt catalyst for SO_2 oxidation. However, chemical discharge with both SO_2 and H_2S are viable options. Use of SO_2 would require an acid removal unit, while use of H_2S requires either filtration or decantation of the floating sulfur from the electrolyte. SO_2 is more readily available as a by-product of the industry. The traditional production of sulfuric acid from SO_2 already requires the purification of the gas, so utilization of this technology is firstly envisaged with this existing infrastructure.[33,34] In this case the last step of conversion of purified SO_2 to SO_3 and production of H_2SO_4, producing heat, would be replaced to produce hydrogen with a dual-circuit RFB. The main problem in mining industry is the volatile arsenic species, but these are almost completely absent in petroleum refineries, where SO_2 is produced in desulfurization step. In this case the other compounds of the gas are mostly hydrocarbons and CO_2. As these compounds do not react with the positive electrolyte, purification processes in these cases will be simpler.

For H_2S, small amounts of H_2S is produced while producing biogas, so the positive electrolyte of the RFB could be used to scrub the biogas and to produce clean hydrogen. On the other hand, natural gas can contain up to 70–80 vol% of H_2S,[48] so gas fields with high H_2S content are another viable target for the current system. Also in this case the raw feedstock does not contain impurities that would complicate the operation of the dual circuit RFB. So we believe that the dual circuit RFB has some viable industrial applications, especially in the mining and oil industry. The economic viability of the system for each particular case has to be carefully analyzed, depending on the required need for the electricity storage and the predicted utilization of the dual circuit process.

Table 1 Efficiency of the dual circuit redox flow battery system considering either AC or DC electricity used to charge the battery, considering either chemical discharge of the positive electrolyte with N_2H_4, SO_2 or H_2S, or electrochemical discharge with SO_2/V(v) fuel cell (FC), for both HHV and LHV

	N_2H_4	SO_2	H_2S	SO_2, FC
		HHV		
DC	49%	57%	53%	69%
AC	48%	56.%	53%	67%
		LHV		
DC	46%	50%	50%	62%
AC	45%	49%	49%	61%

Conclusions

The recent concept of dual circuit redox flow battery to enhance the energy storage capacity of a redox flow battery system has been implemented with an all-vanadium redox flow battery in a pilot scale. The addition of the secondary circuit allows the system to produce hydrogen when a surplus of elec-

tricity is available. Now the storage capacity is no longer dependent on the volume of the liquid electrolytes, but on the hydrogen storage capability, increasing the flexibility of the system.

The hydrogen generation reactor in a kW scale for indirect hydrogen evolution by V^{2+} solution has been designed and characterized. The reactor was performing satisfactory, at 2.4 kW power with highly charged negative electrolyte. As the design of the reactor is modular, the discharge power can be increased by addition of parallel reactors.

Several options have been considered for indirect discharge of the positive electrolyte. As equal amounts of both positive and negative electrolytes need to be discharged to upkeep the balance of the battery, ideally discharge of both electrolytes would take place at the same rate, and both reactions would be easy to implement. Hydrazine reaction produces only gaseous nitrogen is fast and well suited to balance the battery to enable the study of the hydrogen reactor, but does not make sense economically. Both SO_2 and H_2S can be used to discharge the positive electrolyte, and to effectively neutralize these hazardous chemicals. Hydrogen production efficiencies up to 69% (HHV) can be reached with the system coupled with SO_2 fuel cell, while systems coupled with chemical discharge achieve efficiencies up to 58% (HHV). However, only energy generated in an SO_2/V(v) fuel cell is recoverable as electrical energy, as in other cases the chemical energy is converted to heat. Unfortunately the electrocatalytic performance of the SO_2 oxidation has to be drastically improved to reach reasonable current densities from a fuel cell, as the current system would require a fuel cell of almost half the size of the battery stacks to match the capacity of the hydrogen reactor, and this is unacceptable for an add-on unit that is only utilized when there is a surplus of electricity. Additionally, current design requires expensive catalysts like Pt or Au. Hence, H_2S seems to be the best option despite the lower system efficiency of 53% (HHV), as produced sulfur can be easily separated by filtration or flotation (as it is lighter than the battery electrolyte solution), while separation of sulfuric acid produced in SO_2 oxidation would require a separate dialysis system.

An all-vanadium redox flow battery modified with a dual circuit for hydrogen production and H_2S removal has been shown to be an excellent choice for production of hydrogen, when electricity is cheap, with maximum efficiency of 53% for hydrogen evolution. The proposed concept is indeed green chemistry, as hazardous waste product is eliminated to produce clean hydrogen from renewable electricity.

Acknowledgements

The authors acknowledge financial support from Swiss Federal Office of Energy (SFOE) and EOS Holding SA. This work was performed within the Swiss Competence Center of Energy Research, Heat and Storage (SCCER) framework. P.P. acknowledges the financial support from Fondazione Oronzio e Niccolò De Nora. The group of Prof. Lioubov Kiwi, EPFL, is acknowledged for their help for the BET measurements.

Notes and references

1 *EPRI-DOE Handbook of Energy Storage for Transmission and Distribution Applications*, Electric Power Research Institute, 2003.
2 C. R. Dennison, H. Vrubel, V. Amstutz, P. Peljo, K. E. Toghill and H. H. Girault, *Chimia*, 2015, **69**, 753–758.
3 B. Dunn, H. Kamath and J.-M. Tarascon, *Science*, 2011, **334**, 928–935.
4 J. M. Tarascon and M. Armand, *Nature*, 2001, **414**, 359–367.
5 A. Weber, M. Mench, J. Meyers, P. Ross, J. Gostick and Q. Liu, *J. Appl. Electrochem.*, 2011, **41**, 1137–1164.
6 N. Trung and R. F. Savinell, *Electrochem. Soc. Interface*, 2010, **19**, 54–56.
7 M. Skyllas-Kazacos, M. H. Chakrabarti, S. A. Hajimolana, F. S. Mjalli and M. Saleem, *J. Electrochem. Soc.*, 2011, **158**, R55–R79.
8 A. Parasuraman, T. M. Lim, C. Menictas and M. Skyllas-Kazacos, *Electrochim. Acta*, 2013, **101**, 27–40.
9 J. Noack, N. Roznyatovskaya, T. Herr and P. Fischer, *Angew. Chem., Int. Ed.*, 2015, **54**, 9776–9809.
10 D. Lloyd, E. Magdalena, L. Sanz, L. Murtomäki and K. Kontturi, *J. Power Sources*, 2015, **292**, 87–94.
11 M. Vijayakumar, W. Wei, N. Zimin, V. Sprenkle and H. JianZhi, *J. Power Sources*, 2013, **241**, 173–177.
12 G. Kear, A. A. Shah and F. C. Walsh, *Int. J. Energy Res.*, 2012, **36**, 1105–1120.
13 P. Vanýsek, in *CRC Handbook of Chemistry and Physics*, ed. W. M. Haynes, T. J. Bruno and D. R. Lide, Taylor and Francis Group, LLC, 96th edn, 2016, pp. 5:80–5:89.
14 S. Kim, M. Vijayakumar, W. Wang, J. Zhang, B. Chen, Z. Nie, F. Chen, J. Hu, L. Li and Z. Yang, *Phys. Chem. Chem. Phys.*, 2011, **13**, 18186–18193.
15 V. Amstutz, K. E. Toghill, C. Comninellis and H. H. Girault, Redox flow battery for hydrogen generation, *WO* 2013131838A1, 2013.
16 V. Amstutz, K. E. Toghill, F. Powlesland, H. Vrubel, C. Comninellis, X. Hu and H. H. Girault, *Energy Environ. Sci.*, 2014, **7**, 2350–2358.
17 H. Vrubel and X. Hu, *Angew. Chem., Int. Ed.*, 2012, **51**, 12703–12706.
18 M. D. Scanlon, X. Bian, H. Vrubel, V. Amstutz, K. Schenk, X. Hu, B. Liu and H. H. Girault, *Phys. Chem. Chem. Phys.*, 2013, **15**, 2847–2857.
19 L. Liao, S. Wang, J. Xiao, X. Bian, Y. Zhang, M. D. Scanlon, X. Hu, Y. Tang, B. Liu and H. H. Girault, *Energy Environ. Sci.*, 2014, **7**, 387–392.
20 W. Li, R. Zaffou, C. C. Sholvin, M. L. Perry and Y. She, *ECS Trans.*, 2013, **53**, 93–99.
21 S. Velusamy and T. Punniyamurthy, *Org. Lett.*, 2004, **6**, 217–219.
22 H. Huang, Y. Yu and K. H. Chung, *Energy Fuels*, 2009, **23**, 4420–4425.
23 M. H. Barker, Method and apparatus of a copper powder hybrid redox flow battery for electrical energy storage, *FI* 125195, 2015.

24 S. Heimala and M. Ruonala, Method for the production of metal powder, *WO* 2008017731A1, 2008.
25 T. R. Dulski, *A Manual for the Chemical Analysis of Metals*, ASTM International, Ann Arbor, MI, 1996.
26 H. Vrubel, V. H. Cardozo Verzenhassi, S. Nakagaki and F. S. Nunes, *Inorg. Chem. Commun.*, 2008, **11**, 1040–1043.
27 S. S. Y. Lin, W. J. Thomson, T. J. Hagensen and S. Y. Ha, *Appl. Catal., A*, 2007, **318**, 121–127.
28 E. C. Weigert, D. V. Esposito and J. G. Chen, *J. Power Sources*, 2009, **193**, 501–506.
29 M. C. Weidman, D. V. Esposito, Y.-C. Hsu and J. G. Chen, *J. Power Sources*, 2012, **202**, 11–17.
30 R. J. Hussey and J. Wilson, *Advanced Technical Ceramics Directory and Databook*, Springer, 1998.
31 Standard Thermodynamic Properties of Chemical Substances, ed. W. M. Haynes, T. J. Bruno and D. R. Lide, in *CRC Handbook of Chemistry and Physics*, Taylor and Francis Group, LLC, 96th edn, 2016, pp. 5:4–5:42.
32 J. A. O'Brien, J. T. Hinkley, S. W. Donne and S. E. Lindquist, *Electrochim. Acta*, 2010, **55**, 573–591.
33 H. Müller, *Sulfuric Acid and Sulfur Trioxide in Ullmann's Encyclopedia of Industrial Chemistry*, Wiley-VCH Verlag GmbH & Co. KGaA, 2000, vol. 35, pp. 141–211.
34 H. Müller and H. Müller, *Sulfuric Acid and Sulfur Trioxide in Ullmann's Encyclopedia of Industrial Chemistry*, Wiley-VCH Verlag GmbH & Co. KGaA, 2000, vol. 35, pp. 141–211.
35 J. Jeong, M.-S. Kim, B.-S. Kim, S.-K. Kim, W.-B. Kim and J.-C. Lee, *J. Hazard. Mater.*, 2005, **124**, 230–235.
36 E. T. Seo and D. T. Sawyer, *Electrochim. Acta*, 1965, **10**, 239–252.
37 R. J. Kriek, J. Rossmeisl, S. Siahrostami and M. E. Bjorketun, *Phys. Chem. Chem. Phys.*, 2014, **16**, 9572–9579.
38 C. Quijada, E. Morallón, J. L. Vázquez and L. E. A. Berlouis, *Electrochim. Acta*, 2001, **46**, 651–659.
39 D. S. Aaron, Q. Liu, Z. Tang, G. M. Grim, A. B. Papandrew, A. Turhan, T. A. Zawodzinski and M. M. Mench, *J. Power Sources*, 2012, **206**, 450–453.
40 P. W. T. Lu and R. L. Ammon, *Int. J. Hydrogen Energy*, 1982, **7**, 563–575.
41 J. A. Allen, G. Rowe, J. T. Hinkley and S. W. Donne, *Int. J. Hydrogen Energy*, 2014, **39**, 11376–11389.
42 A. Lokkiluoto and M. M. Gasik, *Int. J. Hydrogen Energy*, 2013, **38**, 10–19.
43 L. Xue, P. Zhang, S. Chen and L. Wang, *Int. J. Hydrogen Energy*, 2014, **39**, 14196–14203.
44 L. E. Brecher, S. Spewock and C. J. Warde, *Int. J. Hydrogen Energy*, 1977, **2**, 7–15.
45 P. Ge, M. D. Scanlon, P. Peljo, X. Bian, H. Vubrel, A. O'Neill, J. N. Coleman, M. Cantoni, X. Hu, K. Kontturi, B. Liu and H. H. Girault, *Chem. Commun.*, 2012, **48**, 6484–6486.
46 B. Hinnemann, P. G. Moses, J. Bonde, K. P. Jørgensen, J. H. Nielsen, S. Horch, I. Chorkendorff and J. K. Nørskov, *J. Am. Chem. Soc.*, 2005, **127**, 5308–5309.
47 T. F. Jaramillo, K. P. Jørgensen, J. Bonde, J. H. Nielsen, S. Horch and I. Chorkendorff, *Science*, 2007, **317**, 100–102.
48 F. Pouliquen, C. Blanc, E. Arretz, I. Labat, J. Tournier-Lasserve, A. Ladousse, J. Nougayrede, G. Savin, R. Ivaldi, M. Nicolas, J. Fialaire, R. Millischer, C. Azema, L. Espagno, H. Hemmer and J. Perrot, Hydrogen Sulfide, in *Ullmann's Encyclopedia of Industrial Chemistry*, Wiley-VCH Verlag GmbH & Co. KGaA, 2000, vol. 18, pp. 429–449.